Study on Elastic Elements Allocation
for Energy-Efficient Robotic Cheetah Leg

Ivan I. Borisov [1,2], Ivan A. Kulagin[1], Anastasiya E. Larkina[1], Artem A. Egorov[1],
Sergey A. Kolyubin[1] and Stefano Stramigioli[1,3]

Abstract— The biomimetic approach in robotics is promising: nature has found many good solutions through millions of years of evolution. However, creating a design that enables fast and energy-efficient locomotion remains a major challenge. This paper focuses on the development of a full leg mechanism for a fast and energy-efficient 4-legged robot inspired by a cheetah morphology. In particular, we analyze how the allocation of flexible elements and their stiffness affects the cost of transport and peak power characteristics for vertical jumps and a galloping motion. The study includes the femur and full leg mechanism's locomotory behavior simulation, capturing its interaction with the ground.

I. Introduction

Wheel-based mobile robots are used in many applications providing advantages, such as low energy consumption, high forward speed, and precision. Additionally, they are much easier to construct and control. They have nevertheless lack of versatility, especially for a priori undefined generic terrain. A quadruped robot is an alternative solution and our current research centers on high speed and energy-efficient running of legged robots. The focus of this paper is on the biomimetic legged locomotion and development of an energy-efficient cheetah robot.

The main direction of our research is to find ways to reduce cost of transport of legged locomotion. This is defined as the ratio of the energy spent E to the product of weight W and covered distance d (CoT):$= E/Wd$ [1].

The cheetah is the fastest animal on Earth, which makes it an interesting source of inspiration. There are several advanced robotic platforms trying to mimic its features. We mention here just a few, closely related to our study. The design principles for the energy-efficient legged locomotion and implementation on the MIT Cheetah Robot is presented in [1]. Using energy storage elements to reversibly store the negative work performed during a running cycle and achieve better energy efficiency is described in [2].
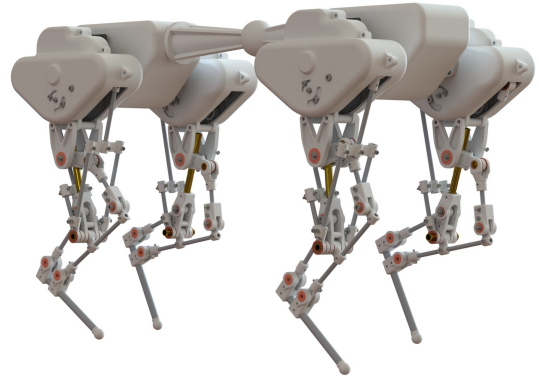
Fig. 1. A render of the proposed design of 4-legged cheetah-robot from the Biomechatronics and Energy-Efficient Robotics Lab, ITMO University

In [3] authors have proven that the cheetah locomotion can be described as a SLIP (spring-loaded inverted pendulum) model. Many walking and running legged robots have fully actuated joints to induce locomotion and this result in complicated control algorithms. An alternative way is to create a system with embedded mechanical intelligence: its desired behavior is programmed by a mechanical design, and simple controllers are sufficient and efficient.

Implementation of motor control for jumping and landing, which exploits the synergy between the control and mechanical structure for a pneumatically actuated bipedal robot called "Mowgli" with an artificial musculoskeletal system, is presented in [4]. The design principles of a highly dynamic biped robot with mechanically adjustable series compliance are described in [5]. An asymmetric antagonistic actuation scheme characterized by large energy storage capacity that enables efficient execution of motions for single degree-of-freedom knee-actuated hopping robot is presented in [6].

This paper is mostly inspired by the robotic cheetah project at the University of Twente[7], [8]. The original task was to create a leg mechanism for a cheetah robot, which is able to run with the least amount of control. These works mostly cover the hip subsystem (femur) development and its analysis. We advance this study to a cheetah-like full leg design and its analysis towards designing a 4-legged robot, which is shown in Fig. 1. As the following analysis shows, the full leg can achieve higher acceleration and speed as well as provide more variability of different walking and running gaits keeping the CoT characteristic close the one of the Minitaur mechanism.
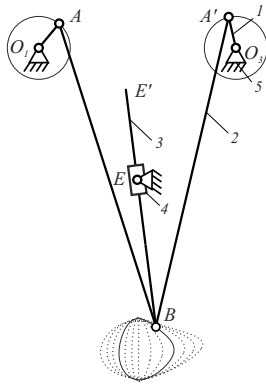
Fig. 2. The femur mechanism of the cheetah robot leg along with their change in trajectory. (1) cranks, (2) connecting rods, (3) crank arm, (4) brick, (5) frame, *B* is a point to be attached with elastic element

We suggest adding elasticity for light-weight parallel kinematics legs as the key factor for better energy-efficiency of the entire system. The challenge is finding the best position and parameters for such elements. This task becomes non-trivial because of the multiple-link structure.

The rest of the paper is organized in as follows. Section II gives a description of the cheetah robot and leg mechanisms evolved from the femur to full assembly. Section III explains how the simulation model was created for the mechanism itself and for actuator dynamics and discusses results of analysis of the femur and full leg structures for different simulation scenarios like vertical jumps and a galloping free run. The jumping height, distance covered within 20 seconds, and CoT for the femur mechanism, which based on the structure called "Minitaur", and for the full leg are presented for various cases of flexibility allocation.

II. MECHANISM DESIGN DESCRIPTION

A. Desired behavior

Let us consider a real cheetah galloping gait. It has a rotary gallop, in which the feet touche the ground in a circular pattern [9]. When a rear foot touches the ground, the knee joint bends to absorb the impact force. Then the legs push the body to the flight phase taking the body forward over the rear leg.

The rear and front cheetah legs look different and have different functions. The rear legs are more muscular than the front and they are mostly responsible for the push off motion. As for the front legs, their main function is to keep the body at a certain distance from the ground. In any case, most of leg muscles are located close to the body to reduce the inertia of the legs as much as possible, while a lot of propulsion comes from elasticity of tendons, muscles and even bones bending.

Trying to mimic these features and reproduce animals running abilities, we should design robot legs as light-weight, but stiff structures with the center of mass strongly shifted towards the hip rotary joint and small feet that can follow variable-shaped trajectories. Embedded elasticity is also a strict requirement.
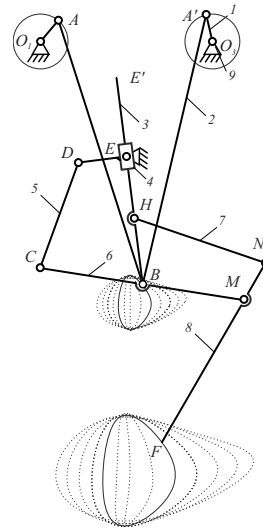

Fig. 3. The mechanism of the leg along with their change in trajectory. (1) cranks, (2) connecting rods, (3) crank arm, (4) brick, (5) sartorius, (6) tibia, (7) fibula, (8) metatarsal, (9) frame, *F* is a foot

B. Prior art in femur mechanism design

The goal is to design a simple planar leg mechanism with a minimal number of actuators and links, able to change the trajectory of the foot by switching between jumping in place and fast running.

A good candidate for this goal is the Minitaur mechanism firstly used in Ghost Robotics Minitaur Quadruped Robot [10]. [8] also suggests using the "Minitaur" structure for the femur mechanism (Fig. 2). The main difference is that the mechanism in [8] has two constantly rotating cranks, compared to pulsing aligned inputs of the Ghost Robotics design, and the leg's actuation principle is based on the resonance of an elastic element attached to the point *B* (Fig. 2).

In this case, the femur structure represents a crank-slider mechanism attached to another mirrored crank-slider mechanism in a slider revolute joint *B*. The cranks AO_1 and AO_3 (1) rotate against each other. The mechanism has two degrees of freedom (DOF). 1 DOF is used to actuate the mechanism, the second DOF is needed to change the phase between the cranks. When the cranks move identically, the slider *B* joint travels vertically in a straight line, but if there is a phase difference between the cranks, the step size increases. A mechanism with a crank arm *BE* and brick *E* is needed as a guideline for an elastic element.

In general the Minitaur mechanism has several advantages. It can change the step size via adjusting an angle between cranks, it is able to provide a smooth push motion of a foot during a stance phase (when the foot touches the ground) and to retract itself as close to the body as possible during the flight phase to decrease the rotational inertia of the leg to save the energy. However, the main advantage of the Minitaur is that the vertical displacement is almost uncoupled from the step size. The vertical size is almost the same for all output trajectories (see Fig. 2).

1697

C. Full leg mechanism design

In [8] a foot mechanism was not studied. Instead, an elastic element was used to absorb the impact forces, also employing a passive energy storage. In contrast, our paper elaborates the idea to create a more cheetah-like full leg mechanism, which is able to provide the faster acceleration and speed. Here, we describe a full leg design based on the "Minitaur" structure and real cheetah anatomy.

Following a cheetah anatomy, a tibia, a fibula, and a metatarsal should be added to the Minitaur femur mechanism to create a full leg structure. The full leg mechanism has been designed using three position synthesis method as an assembly of the Minitaur, two rockers 4 bar mechanism $HNFNB$, and a rocker-slider mechanism $BCDE$. (see Fig. 3). A 4 bar rocker-slider mechanism $BCDE$ was added as a knee. The slider brick E is fixed with DE, the link DC is a connecting rod, CB is a rocker in the description of a rocker-slider mechanism or the tibia in the description of a cheetah leg structure. The two rockers 4 bar mechanism was added as an ankle. In the description of a 4 bar mechanism, BM and HN are rockers, HB is a frame, NMF is a connecting rod. In the description of the cheetah leg BM is the second part of the tibia, HN is a fibula, and NMF is a metatarsal.

The changes in the trajectory between points B and F can be seen in Fig. 3. It can be observed that the foot mechanism acts as a motion converter, while the ratio between both trajectories equals 2. As a result, the gait can be twice wider and twice higher resulting in higher speed of locomotion.

In terms of actuation, the idea is to use one powerful DC motor to rotate both cranks of the mechanism and an additional servo motor to control the phase between the cranks. The movement translation from the main DC motor to both cranks can be implemented via a planetary gearbox. Thus, the leg mechanism can be divided into a linkage mechanism and a planetary gearbox.

III. SIMULATION-BASED MECHANISM ANALYSIS

As mentioned above, a leg mechanism has to store and release mechanical energy as well as soften impact shock during the galloping motion, therefore, it is to be equipped with elastic elements. For a Minitaur the allocation of a spring seems quite obvious, but it is really a question in terms of the full leg mechanism.

Let us consider how to make the best design choices for the allocation of elastic elements and their parameters based on a dynamic simulation analysis.

A. Model Description and Simulation Scenarios

A detailed simulation is a good tool to evaluate and support fundamental design choices, study interaction between different parts of a complicated mechanical structure and environment, and further plan reference trajectories and tune controllers [11]. Since a mechatronic system is an interaction between mechanics, electronics, and information, simulation should be performed with respect to all domains. In order to do that, we have implemented a simulation in MATLAB Simscape Multibody using Contact Forces Library.
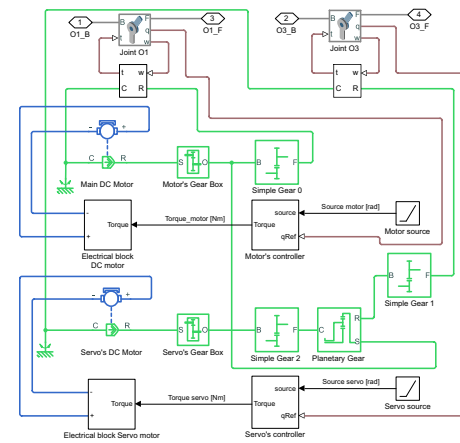

Fig. 4. The actuators block consisting of 2 revolute joints, gearbox, DC motors, electrical, and controllers blocks with the sources of input signals

The mechanisms' models were implemented according to the kinematic schemes shown in Fig. 2 and Fig. 3. The robot is considered as a planar mechanism connected with a world frame with a rectangular joint. This means it is able to jump in place or run along a horizontal line. Links were modeled as rigid bodies using solid blocks combining a geometry, inertia and mass, graphics component, and rigidly attached frames into a single unit. The inertia tensors were obtained from the link geometry assuming uniform material density distribution. The planetary gearbox is implemented via Matlab Simscape Driveline. The model designed also allows to capture leg-ground dynamic interaction using the penalty-based approach for contact modeling [12]. For better models of spatial visco-elastic contacts [13] can be used.

The phase control between the cranks is essential for the reconfiguration of the mechanism for the trajectory changing. The simulation was conducted for the Minitaur and the full leg with various elastic elements allocation with the wide range of phases in order to understand what design is better in terms of jumping height, speed, and energy efficiency.

B. Actuator model

The model of an actuator block is shown in Fig. 4. There are two rotational joints O_1 and O_3, which actuate the cranks. The joint O_1 is connected via Simscape Interface to one of the two the gears of the *Simple Gear 0*. The *Main DC Motor* transmits the motion to the second gear of *Simple Gear 0* via *Motor's Gear Box*. The shaft of the *Motor's Gear Box* is attached to a sun gear S of the *Planetary Gear*. The second revolute joint O_3 is connected to a small gear of the *Simple Gear 1* block. The bigger gear of the *Simple Gear 1* (ratio equals to 1/3) is fixed with the planetary gearbox's ring R (ratio equals to 3). The additional servo motor transmits the motion through a *Servo's Gear Box* and a *Simple Gear 2* to a Carrier C of the *Planetary Gearbox*. Thus, we obtain the same motion on both cranks, with the phase being controlled via a servo motor. To control the positions of the cranks two PID controllers are implemented for the servo and the DC motor respectively. Control torques are calculated
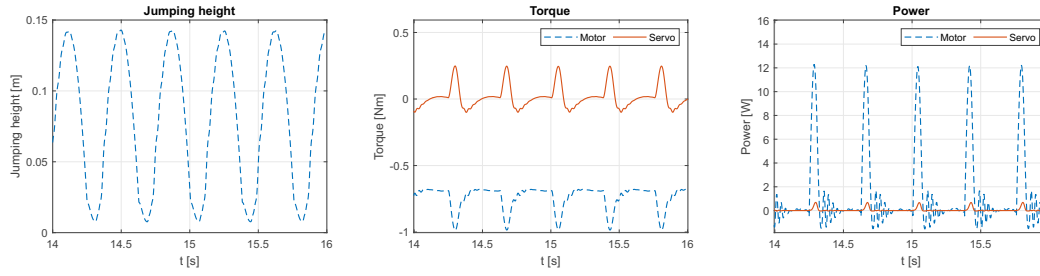
Fig. 5. Simulation results for jumping in a place of the femur mechanism "Minitaur" ($K_1 = 1.8 \frac{N}{mm}$)

based on the difference between the desired and computed motor's and servo's angles and then sent into electrical blocks modeling the PWM transformer and the H-Bridge. Then calculated voltages are fed to both drives. This additional model, which takes into account electromagnetic effects, is important because of two reasons. At first, this is the way to estimate the electrical energy consumed, which influences batteries capacity. Moreover, it enables direct calculation of voltages and currents that are efforts and flows within the port-Hamiltonian approach framework, which is planned to be used later for energy-aware motion controllers design.

C. Femur mechanism case study

As the first step of the simulation let us consider the Minitaur femur mechanism, which represent a typical SLIP model. In order to achieve the hopping behavior, a spring has to be attached to the joint *B*, since it is a symmetrical structure. If the hopping in a place is a desired behavior, the phase between cranks must be zero. Otherwise, the robot starts to run.

In order to model impacts between the mechanism and the ground surface we have implemented a penalty force approach, which allows a small overlap of the bodies, using the MATLAB's Contact Library. The simulation results for jumping in place for the Minitaur is presented in Fig. 5. The vertical position sensor is attached to the center of a contact sphere, which is connected to a contact point. Therefore, it shows values above zero at the lowest impact position for the jumping height plot. Within the context of this work, the most interesting characteristic is the power consumption. For the example selected its peak value is almost 12 *W* per impact. As seen, the servo power is quite small, since the servo is only responsible for phase changing; it means impact forces do not affect a moving low-inertia part.

The simulation was conducted for a wide range of phases from -2.9 *rad* to 2.9 *rad*, with various spring stiffness and damping coefficients. Step size is 0.26 *rad*. Free-run experiments are worth making a closer look at. The running sequence is shown in Fig. 6, (a). They revealed that a stable behavior is possible within a narrow range of coefficients. The results of the free-run scenario simulation with the spring stiffness coefficients $K_1 = 1.8 \frac{N}{mm}$, $K_2 = 1.6 \frac{N}{mm}$, $K_3 = 1.6 \frac{N}{mm}$ and damping $\beta = 1\frac{N}{m/s}$ are shown in Fig. 7. The spring natural length is 5 *cm*. The main mass is concentrated in the robot's body, the total robot mass equals 0.875 *g*.

The first plot shows the relation between the phase and the jumping height. It can be seen that the height is stable and almost uncoupled to the phase. The stable jumping height is almost 14 *cm*. The second plot shows the distance covered within 20 seconds of the simulation; the maximum horizontal velocity is approximately 1 *m/s*. The third plot is the relation between CoT and the phase. The CoT is the ratio of the spent energy to the product of weight and covered distance. CoT decreases with the increasing in phase, because of the greater distance. If the distance is almost zero (jumping in a place) than the CoT tends to go to infinity.

D. Leg mechanism case study

When the whole leg mechanism has to be designed, one of the tasks is to understand where an elastic element should be located to obtain the best characteristics in terms of the jumping height, horizontal velocity and energy efficiency.

Evolving from the femur mechanism to the full leg mechanism, only four links were added. Since link 6 *CM* acts as a tibia it has to be rigid to hold external forces. Therefore, only three links remain candidates to be replaced by flexible elements: either a spring-damper with a guide or a flexible link. Namely, rising parallels with cheetah anatomy, we consider the following cases (see Fig. 3):

1) Link *MF* can be considered as a metatarsal, it can be studied as a flexible body, while others links are rigid bodies.
2) Link *DC* can be considered as sartorius and built as a spring on a prismatic joint, while others links are rigid bodies.
3) Link *HN* can be presented as a fibula and built as a spring on a prismatic joint, while others links are rigid bodies.

1) Metatarsal-allocated flexibility: As the second step of the simulation let us analyze the full leg simulation results with a metatarsal-allocated flexible link (Fig. 6, b). The simulation was performed for different materials as nylon (Young's modulus $E = 2\,GPa$, Poisson's ratio $v = 0.39$), rubber ($E = 0.5\,GPa$, $v = 0.48$), and glass fiber ($E = 72\,GPa$, $v = 0.21$). Corresponding simulation results are shown in Fig. 7. These results are similar to the Minitaur: the narrow region of jumping in the middle, it is able to run forward and backward (but these areas are reversed), jumping height is almost uncoupled with the phase. However, since there is not
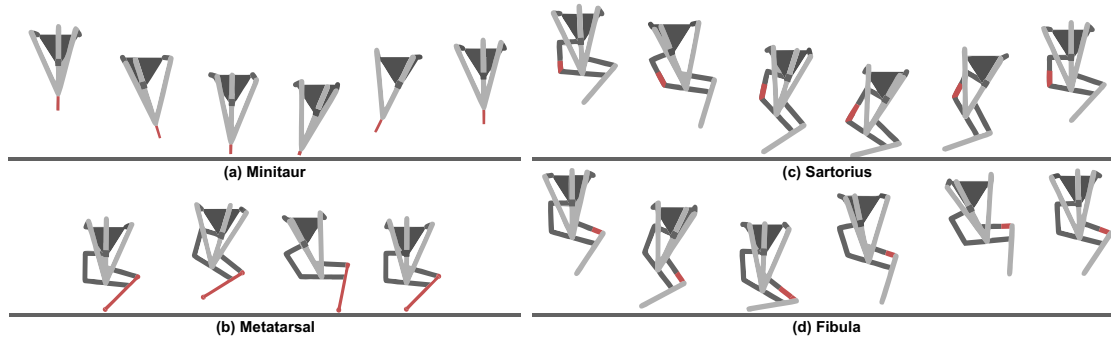
1699

Fig. 6. Animation of the running sequence for free-run of the femur mechanism "Minitaur" (a), free-run of the full leg mechanism with metatarsal-allocated flexibility (b), sartorius allocated flexibility (c), and fibula-allocated flexibility (d). The red element indicates an elastic element
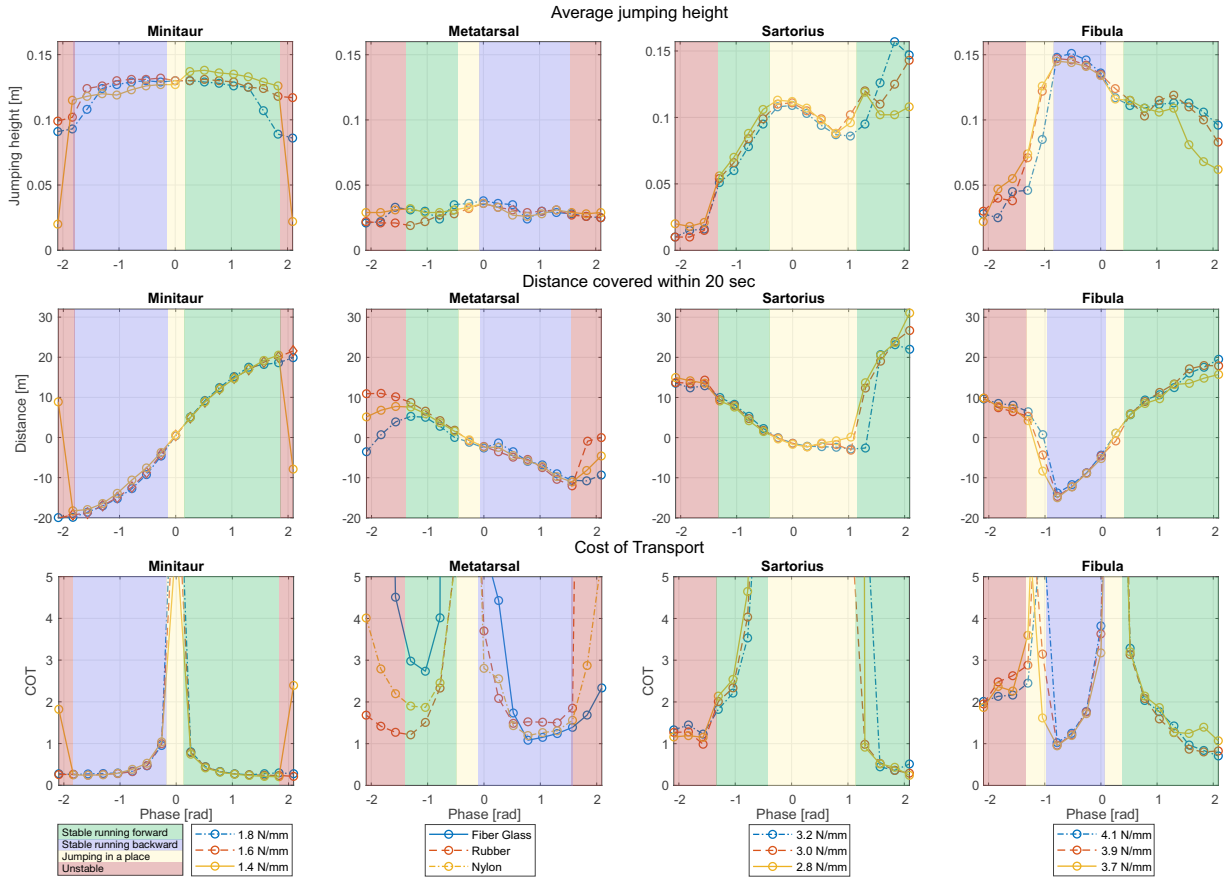

Fig. 7. The simulation results show relation between the jumping height, distance covered within 20 second, cost of transport criterion and the phase between the cranks. The yellow area indicates stable jumping in a place with a relativity small horizontal velocity, the green area means running forward, the violet area displays running backward, and the red zone means unstable behavior

enough elasticity in the system the jumping height is very small and CoT for flexible metatarsal is too high. It leads to the conclusion that the use of one flexible link without additional springs is insufficient.

2) Sartorius-allocated flexibility: Now let us consider the running of the whole leg mechanism with a spring on a prismatic joint, which is located inside the link *DC*, which we call 'sartorius' (Fig. 6, c). The simulation was also performed within a range of spring stiffness coefficients from

$K_1 = 3.2 \frac{N}{mm}$ through $K_2 = 3.0 \frac{N}{mm}$ until $K_3 = 2.8 \frac{N}{m}$ with the same damping coefficient $\beta = 1 \frac{N}{m/s}$. The natural length of the spring is 3.5 *cm*. Corresponding simulation results are shown in Fig. 7. It was concluded that the behavior is significantly different comparing with Minitaur and Metatarsal-allocated flexibility. It has a very wide area for jumping in a place and a very short transition region to the running mode. It is hopping in a place if the phase equals 1.04 *rad*, but if will change it a little bit and make it 1.3 *rad* than the robot will
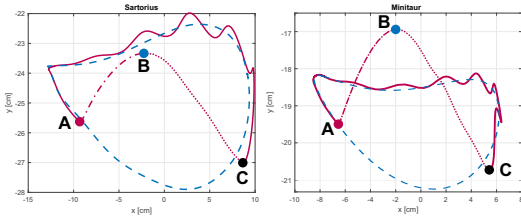
1700

Fig. 8. The trajectories of a contact point with the ground for the Sartorius-allocated flexibility and the Minitaur femur mechanism in bodies frames

run at 0.7 m/s. The maximum horizontal velocity is 1.5 m/s if the phase is 2.09 rad, which is much faster comparing to the Minitaur.

The main disadvantage is that we got lacks in controllability. If we want slower velocity we have to change the sign of the phase, since instead of backwards movement there is a different gait for the forward moving.

Fig. 8 shows the trajectories of a contact point with the ground for the Sartorius-allocated flexibility and the Minitaur femur mechanism in bodies frames. The blue dashed lines show the trajectories without contact modeling as in Figures 2 and 3. The red lines are the trajectories of the contact points with contact modeling. Point A indicates the initial moment of contact, point B indicates the takeoff. The dashed-dotted curve AB describes the spring compression, the dotted curve BC means disclosure of the spring. In order to get the stable running behavior the trajectory must be similar to the depicted trajectories.

3) Fibula-allocated flexibility: Finally, we have simulated the leg mechanism with a spring located inside the link HN, which we call 'fibula' (Fig. 6, d). The simulation was also conducted with a range of stiffness coefficients from $K_1 = 4.1 \frac{N}{mm}$ through $K_2 = 3.9 \frac{N}{mm}$ until $K_3 = 3.7 \frac{N}{mm}$ and damping coefficient $\beta = 1 \frac{N}{m/s}$. The natural length of the spring is 3.5 cm. Corresponding simulation results are shown in Fig. 7. The behavior is much better that metatarsal-allocated flexibility, but much worse than the Minitaur. The controllability is better in previous example. However, it does not have any advantages comparing with the Minitaur.

IV. CONCLUSION AND FUTURE WORK

The paper presented the analysis of the Minitaur femur mechanism and the cheetah-inspired full leg structure for a energy-efficient galloping motion. The femur mechanism from [8] was considered in the paper as a benchmark that should be outperformed by the proposed full leg design.

We have discussed the galloping robot leg structures inspired by cheetah morphology and studied the best flexibility allocation for it. To do so we performed extensive simulations considering three major scenarios (metatarsal-, sartorius-, and fibula-allocated flexibility) for a wide range of phase differences, stiffness and damping coefficients as well as natural lengths for spring elements or Young's modulus and Poisson's ratio for flexible beams. Simulation models have been developed using the MATLAB Simscape Multibody package with the Contact Forces Library for leg-ground

contact modelling. It was concluded, that the best design in terms of horizontal velocity and energy efficiency is the sartorius-allocated flexibility with stiffness coefficient $K_3 = 2.8 \ N/mm$, actual damping coefficient $\frac{\beta = 1}{Nm/s}$, and phase difference 2.09 rad. Modelling taking into account real mass distribution, body inertia, and drives' dynamics shows that such a leg is able to run with the highest achievable velocity given assumed design constraints of up to 1.5 m/s with the best achievable among all considered cases CoT = 0.3, which is comparable with the best-in-class results for actuated legged robots reported in [1].

As the next step to make the quadruped design following the cheetah morphology we are planning to experiment with front and rear legs' mechanisms and focus on motion synchronization and control.

ACKNOWLEDGMENT

REFERENCES

[1] S. Seok, A. Wang, M. Y. (Michael) Chuah, D. J. Hyun, J. Lee, D. M. Otten, J. H. Lang, and S. Kim, "Design principles for energy-efficient legged locomotion and implementation on the mit cheetah robot," *IEEE/ASME Transactions on Mechatronics*, vol. 20, no. 3, pp. 1117–1129, June 2015.

[2] G. A. Folkertsma, S. Kim, and S. Stramigioli, "Parallel stiffness in a bounding quadruped with flexible spine," in *2012 IEEE/RSJ International Conference on Intelligent Robots and Systems*, Oct 2012, pp. 2210–2215.

[3] H. Yu, M. Li, W. Guo, and H. Cai, "Stance control of the slip hopper with adjustable stiffness of leg spring," in *2012 IEEE International Conference on Mechatronics and Automation*, Aug 2012, pp. 2007–2012.

[4] R. Niiyama, A. Nagakubo, and Y. Kuniyoshi, "Mowgli: A bipedal jumping and landing robot with an artificial musculoskeletal system," in *Proceedings 2007 IEEE International Conference on Robotics and Automation*, April 2007, pp. 2546–2551.

[5] J. W. Hurst, J. E. Chestnutt, and A. A. Rizzi, "Design and philosophy of the bimasc, a highly dynamic biped," in *Proceedings 2007 IEEE International Conference on Robotics and Automation*, April 2007, pp. 1863–1868.

[6] W. Roozing, Z. Li, G. A. Medrano-Cerda, D. G. Caldwell, and N. G. Tsagarakis, "Development and control of a compliant asymmetric antagonistic actuator for energy efficient mobility," *IEEE/ASME Transactions on Mechatronics*, vol. 21, no. 2, pp. 1080–1091, April 2016.

[7] G. Folkertsma, "Energy-based and biomimetic robotics," Ph.D. dissertation, University of Twente, Netherlands, 4 2017.

[8] M. Snippe, "Cheetah robot leg mechanism: analysis, design and cost of transportt," Netherlands, 6 2017.

[9] J. E. Bertram and A. Gutmann, "Motions of the running horse and cheetah revisited: fundamental mechanics of the transverse and rotary gallop," *Journal of the Royal Society Interface*, vol. 6, no. 35, pp. 549–559, 2008.

[10] G. Kenneally, A. De, and D. E. Koditschek, "Design principles for a family of direct-drive legged robots," *IEEE Robotics and Automation Letters*, vol. 1, no. 2, pp. 900–907, 2016.

[11] R. Hyde and J. Wendlandt, "Tool-supported mechatronic system design," in *2008 34th Annual Conference of IEEE Industrial Electronics*. IEEE, 2008, pp. 1674–1679.

[12] C. Rengifo, Y. Aoustin, C. Chevallereau, and F. Plestan, "A penalty-based approach for contact forces computation in bipedal robots," in *2009 9th IEEE-RAS International Conference on Humanoid Robots*. IEEE, 2009, pp. 121–127.

[13] S. Stramigioli and V. Duindam, "Port based modeling of spatial visco-elastic contacts," *European Journal of Control - EUR J CONTROL*, vol. 10, 12 2004.